EPJ Web of Conferences **37**, 01008 (2012)
DOI: 10.1051/epjconf/20123701008

Final State Interactions and Polarization Observables in the Reaction $pp \to pK\Lambda$

Matthias Röder[a] and James Ritman for the COSY-TOF Collaboration

Institut für Kernphysik, Forschungszentrum-Jülich GmbH

Abstract. Due to the lack of high quality hyperon beams, final state interactions in hyperon production reactions are a compelling tool to study hyperon-nucleon interactions. The COSY-TOF experiment has recently been upgraded in order to reconstruct the $pK^+\Lambda$ final state with sufficient precision to determine the spin triplet $p\Lambda$ scattering length with a polarized proton beam. We find an unexpected behavior of the K^+ analyzing power which prevents the extraction method to be used with the available statistics. A theoretical explanation is pending. Furthermore, the polarized beam together with the self analyzing decay of the Λ allows us to determine the Λ depolarization. This is especially sensitive to K^+ and π exchange in the production mechanism. Our finding verifies, to a large extent, the result from DISTO [2] that has so far been the only measurement close to the production threshold.

1 Introduction

An important part of the current strangeness physics program of the COSY-TOF collaboration is the study of the reaction $pp \to pK\Lambda$. One goal is to study the $pK\Lambda$ production mechanism with polarization observables that are accessible with the polarized proton beam and self analyzing decay of the polarized hyperon. Here, we focus on the spin transfer coefficient D_{NN} that is sensitive to π or K exchange. Another objective is to study hyperon nucleon interactions in $p\Lambda$ final state interactions which is a is a compelling tool due to the lack of high quality, low energy hyperon beams. In Ref. [1] a method was proposed to extract the effective $p\Lambda$ scattering length (a_e) from the *shape* of the final state interactions in the proton-lambda invariant mass spectrum. This allows us to extract the spin triplet scattering length (a_t) with the help of the K Analyzing power (A_N).

2 Experimental Setup

Recently, the COSY-TOF detector has been upgraded to measure the $p\Lambda$ scattering length with a precision that competes with the theoretical error. The tracking capabilities were significantly improved with a Silicon Quirl close to the target and a Straw Tube Tracker (STT) inside the COSY-TOF vacuum vessel.

Because the final state particles (green lines) have momenta in the order of a few hundred MeV it is crucial for precise event reconstruction to minimize multiple scattering. The radiation length is approximately $0.02\,X/X_0$ before a particle hits the segmented scintillators at the inner side of the barrel or the end caps. Together with the start scintillators close to the target they are primarily used for the trigger, time of flight measurement with $\sigma = 200$ ps resolution and the determination of specific energy loss.

The spatial reconstruction precision is dominated by the STT with 2704 straw tubes arranged in 26 layers. These are grouped into densely packed double layers that are consecutively rotated by 60 deg

[a] e-mail: m.roeder@fz-juelich.de

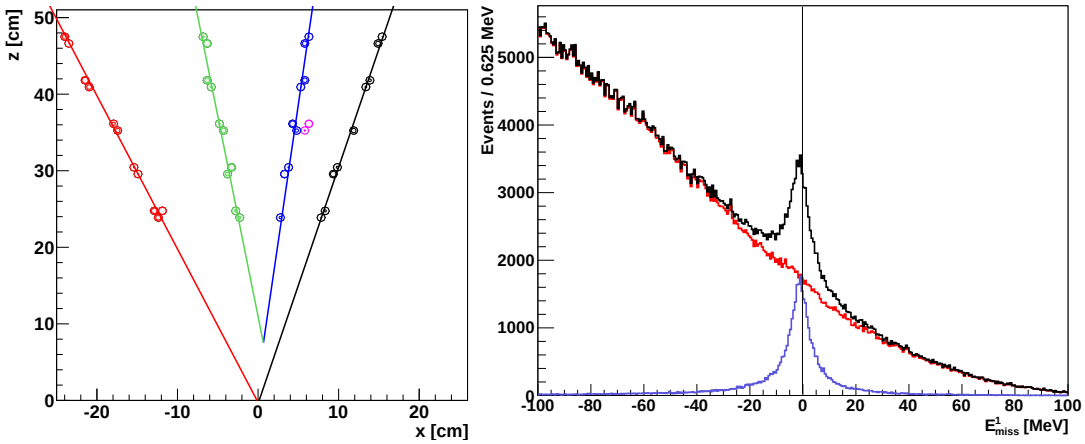

Fig. 1. Left: An event display of one of three STT orientations. The large circles mark the straw outer diameter and the smaller inner circles mark the measured track to wire distances. Right: The missing energy in the primary vertex before the kinematic fit. For all events a longer Λ flight path than 1 cm (black) and the event selection (blue) as described in the text. Also the difference (red) is shown.

for three dimensional track reconstruction. The mylar walls are only 20μm thick. To achieve stability while avoiding material for support structures the 20/80 Ar/CO_2 drift gas mixture is kept at 1250 mbar overpressure compared to the COSY-TOF vacuum. Because the STT delivers between 8 and 35 hits for each final state particle it is the most important detection subsystem for the analysis. Especially, the delayed hyperon decay vertex can be reconstructed.

In the following, one week beam time with stable beam polarization at a beam momentum of $p_b = 2.95\,\mathrm{GeV}/c$ is beeing analyzed.

3 Event Reconstruction and Selection

The event reconstruction starts with a Hough transformation for two dimensional track finding in each of the three STT orientations. These tracks are combined to three dimensional tracks and optimized with MINUIT. The average spatial reconstruction precision is found to be 150 μm. Events with 4 reconstructed tracks are selected. These are checked and optimized to match the $pK\Lambda$ event geometry: A delayed two prong vertex, where the decay plane contains a primary two prong vertex at the target position. The spatial resolution of the primary vertex position along the beam axis is found to be $\sigma_z \approx 1$ mm. This is important to reject background events with four charged primary tracks like $pp \to pp\pi^+\pi^-$. A minimum of 3 cm flight path in the laboratory system to the secondary vertex is chosen as a threshold.

For the maximum possible reconstruction precision a kinematic fit is performed that optimizes the event kinematics with respect to the residuals of the STT's track to wire distances. This is depicted in Fig. 1 left. The selection on the reduced $\chi^2_K < 5$ also suppresses the physical background process $pp \to pK\Sigma^0 \to pK\Lambda\gamma$. Because the photon carries away no more than 70 MeV, the event topology is similar to signal events if the photon is not detected. Monte Carlo based studies showed that the final physical background contamination is below 5 %. Also the K and p identification is based on the resulting χ^2 of both hypotheses. The Λ decay particles are indentified by kinematical constraints.

To test the event selection we calculate the four-momenta of p, K and Λ from the initial state four momentum, the reconstructed track directions and momentum conservation. The resulting missing energy is given in Fig. 1 on the right. All events with a converged kinematic fit and a hyperon flight path longer than 1 cm are shown in black. The above mentioned selection criteria leave the events shown in blue in the event sample. The difference is shown in red.

Studies with Monte Carlo Simulated events have shown that the reconstruction efficiency for the charged final state in the reaction $pp \to pK\Lambda \to p\pi$ is 20%. The $p\Lambda$ invariant mass resolution is

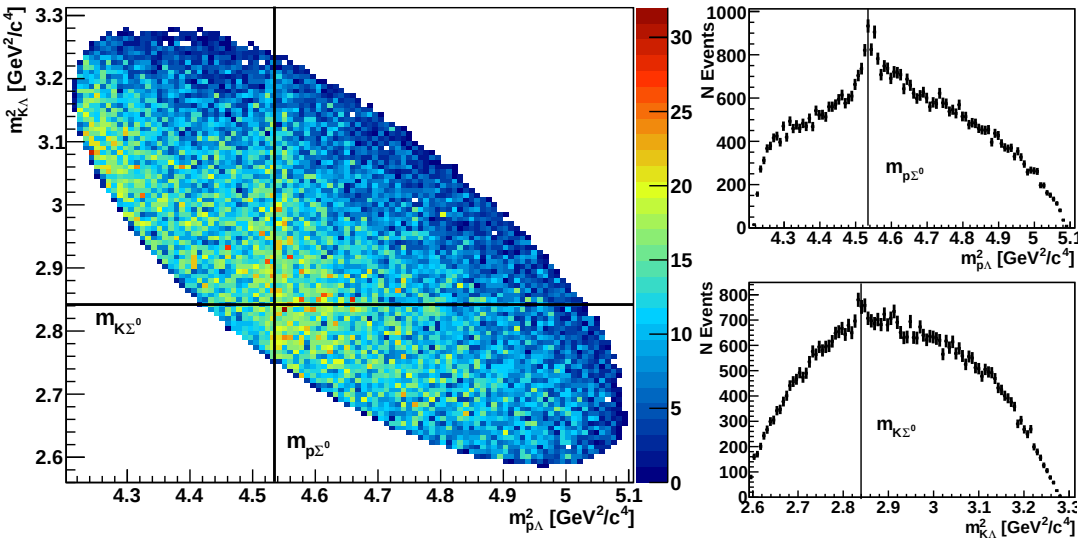

Fig. 2. The dalitz plot (left). The lines mark the $p\Sigma^0$ and $K\Sigma^0$ thresholds, respectively. The projections on $m^2_{K\Lambda}$ (top) and $m^2_{p\Lambda}$ (bottom) are also shown on the right.

$\sigma_m \approx 1\,\mathrm{MeV}/c^2$. The importance of the STT for the measurement is obvious considering that this is a factor of four improvement over the previous COSY-TOF.

The Dalitz plot of the selected 42,000 events not yet corrected for reconstruction efficiency is shown in Fig. 2 on the left. One sees that the detector has full kinematical acceptance and that the high resolution reveals several structures. In $m^2_{p\Lambda}$ there is a clear cusp at the $p\Sigma^0$ threshold. The exact peak position and peak shape that will be subject to further studies of the corresponding coupled channel effect. In the projection on $m_{K\Lambda}$ on the bottom right we also find indications for a cusp structure at the $K\Sigma^0$ threshold. The underlying structure of the Dalitz plot can be explained by final state interactions and N^* resonances.

4 Polarization Observables

The Λ polarization is determined from the asymmetry of the decay. In agreement with previous studies at COSY-TOF we find, with the weighted sums method [3], +10% polarization for backward and -10% polarization for forward Λs. From the asymmetry of pp elastic scattering the beam polarization is determined to be $(61.0 \pm 1.6)\%$. The influence of the beam polarization on the lambda polarization is quantified by the spin transfer coefficient D_{NN}, also called depolarization. It is determined by dividing the event sample into four subsamples: One for beam spin up and the quantization axis of the Λ in the same detector hemisphere ($\uparrow\uparrow$) and another for the opposite detector hemisphere ($\uparrow\downarrow$). Additional samples with beam spin down ($\downarrow\downarrow$,$\downarrow\uparrow$) are important to control systematic effects from azimuthal angular asymmetries in the detector acceptance. The corresponding polarizations are shown in Fig. 3 on the left. The depolarization on the right is then simply determined by the differences of the Λ polarization of the four subsamples [2].

The measured polarization values (P) in Fig. 3 clearly deviate from the $\pm 10\%$ observed with unpolarized beam. It is important to note that the results for different beam spin orientation $P^{\uparrow\uparrow}$, $P^{\downarrow\downarrow}$ and $P^{\uparrow\downarrow}$ are self-consistent. This indicates that systematic effects of detector asymmetries are below the statistical accuracy of our measurement. The difference between same and opposite detector hemispheres, i.e. D_{NN} becomes larger for forward Λs as can be seen in Fig. 3 on the right. In the forward region we are in agreement with a measurement from DISTO [2]. However, for backward Λs we find a D_{NN} significantly closer to zero.

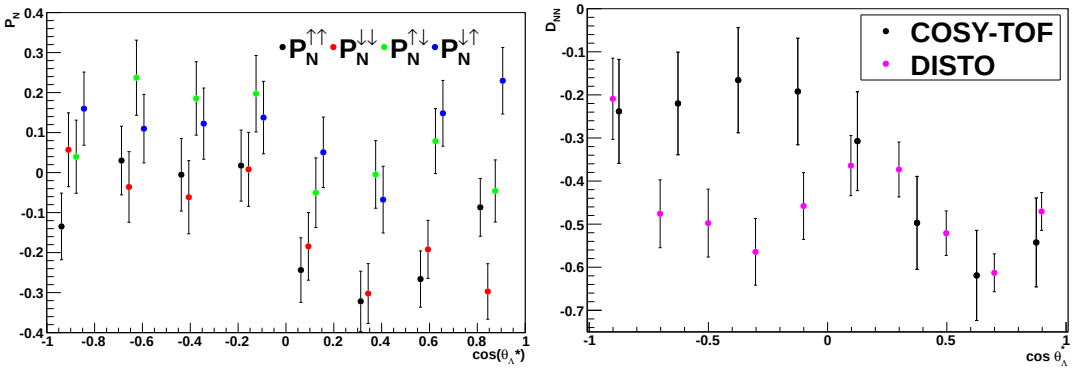

Fig. 3. The measured Λ polarization values for the different event subsamples as described in the text (left). The difference of pairs of samples is quantified by the depolarization D_{NN} (right).

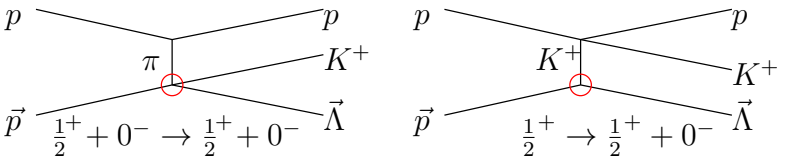

Fig. 4. Meson exchange diagrams in the Laget model [4]. The spin and parity structure for π exchange (left) requires no spin flip in contrast to the K exchange (right) [2].

The Laget model [4] considers π and K exchange as production mechanism. Structures at the Λ production vertex, that are depicted in Fig. 4, require no spin flip for *pi* and a spin flip for K exchange. This corresponds to D_{NN} of +1 and -1, respectively. In this model our finding can therefore be described by a dominant K exchange and a modest contribution of π exchange. The vanishing D_{NN} for backward Λs is expected [2] from models that predict a connection of the Λ and the unpolarized proton target backward and the polarized beam proton forward.

5 Final State Interactions

In Fig. 5 on the left the $p\Lambda$ invariant mass spectrum is given. The number of measured events is corrected for detector acceptance (A). The latter is determined with Monte Carlo simulated events and shown in the bottom. In comparison to the arbitrarily scaled phase space (p'), drawn as solid line, the enhancement due to the final state interactions is obvious. By dividing the data with p' one obtains the effective scattering amplitude squared. Because the luminosity of the event sample is not known, the units are arbitrary. As derived in Ref. [1], by a dispersion relation, one can still extract the scattering length from the *shape* of the amplitude spectrum. For that, an exponential function convoluted with the detector resolution is fit. The data is well described by this as shown by the reduced $\chi^2 = 0.56$. Following the method in Ref. [1] we obtain $a_e = (-1.29 \pm 0.01 \pm 0.03)$ fm.

The next step would be to determine a_t. Because only the shape is needed, it is sufficient to find an observable that is proportional to the spin triplet scattering amplitude. For that, it can be shown [1] that close to threshold only spin triplet scattering contributes to K P-waves. These on the other hand are accessible through the K analyzing power. This quantity is shown in Fig. 6 on the left. It is fit with a partial wave analysis that consists of a symmetric contribution from S and P and an asymmetric contribution from S and D wave interference. These are described by associated Legendre polynomials. The low reduced $\chi^2 = 0.54$ justifies the exclusion of higher partial waves. The next step would be to determine the dependence of the coefficient of the symmetric Legendre polynomial on the $p\Lambda$ invariant mass. However, as shown in Fig. 6 on the right with the red markers, in the region of FSI it is so low that we cannot resolve the $m_{p\Lambda}$ dependence in this area with the present amount of collected data.

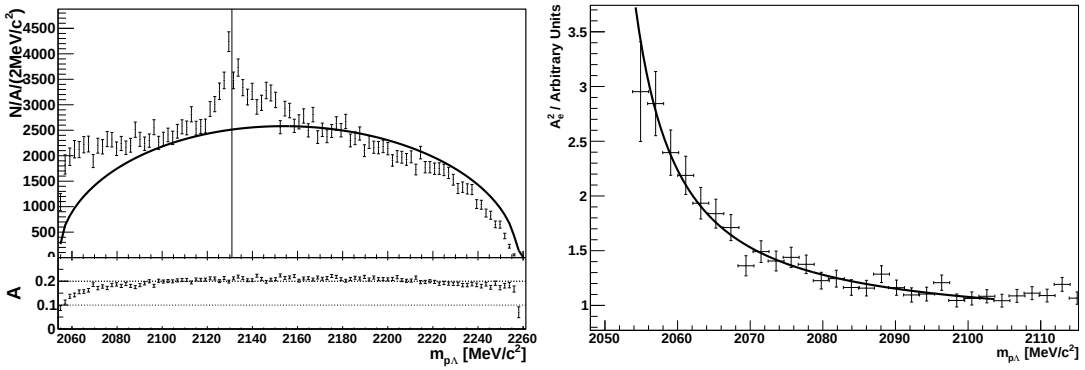

Fig. 5. The $m_{p\Lambda}$ spectrum (left) corrected for acceptance as given on the bottom. The $p\Sigma^0$ threshold is marked and an arbitrarily scaled phase space distribution is given by the solid line. The scattering amplitude (right) is fit by an exponential function to extract a.

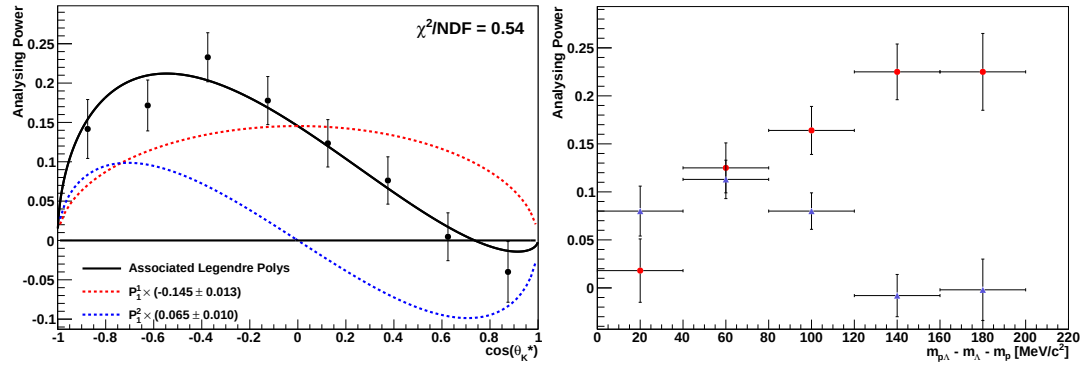

Fig. 6. The K analyzing power (left) is fit with a symmetric (red) and and an asymmetric Legendre polynomial (blue). The dependence of the coefficients on $m_{p\Lambda}$ (right) is given by the same colors.

The measurement of a_e shows that our experimental precision surpasses the systematic uncertainty inherent to the extraction method. Several theories like the Nijmegen potential [5] and Jülich model [6] or chiral effective field theory [7] predict $a_t \approx -1.8$ and $a_s \approx -2.4$. This consensus is driven by the need to predict a bound hypertriton. Naively, one would expect to measure an a_e between these values. Considering the statistic uncertainty our finding is on the low end of this range. This could be interpreted as dominance of spin triplet scattering. However, in the Dalitz plot in Fig. 2 an influence of N^* resonances is apparent. The effect on the measurement remains to be determined. This will be approached by analysing different slices in $m^2_{K\Lambda}$ and at different beam momenta.

The $m_{p\Lambda}$ dependence of the K analyzing power in Fig. 6 on the right was not anticipated because it deviates from measurements of the reaction $pp \to d\pi^+$ with the same selection rules. As expected, the asymmetric contribution decreases with increasing $m_{p\Lambda}$ because the K has not enough momentum for D wave interference. Surprisingly, the symmetric contribution decreases at low $m_{p\Lambda}$. As explained above, close to threshold only spin triplet scattering contributes to the latter. Therefore, this behavior could be explained by its absence. This was also claimed by the Hires collaboration [8]. This would mean that $a_e = a_s$ which Hires measures as $a_s = -2.43^{+0.16}_{-0.25}$. The deviation from our measurement could partly be explained by Ref. [9] that finds a systematic shift for of a by ≈ -0.4 fm when using the Hires method. As mentioned above also N^* resonances could influence either result.

However, other explanations exist: There are several P wave amplitudes that could be individually zero or cancel out. Furthermore, only the imaginary part of S and P wave interference enters the analyzing power. This adds the possibility of a phase cancellation. To check the viability of these it is important to improve the statistics of the measurement.

6 Conclusion

The reaction $pp \to pK\Lambda$ has been measured with full kinematical acceptance, a reconstruction efficiency of 20% and an invariant mass resolution of $\sigma_m \approx 1\,\mathrm{MeV}/c^2$. The data reveals an interesting Dalitz plot structure with a prominent cusp structure in at the $p\Sigma^0$ threshold in the $p\Lambda$ invariant mass and indications of a cups structure at the $K\Sigma^0$ threshold in the $K\Lambda$ invariant mass.

Preliminary results on the Λ depolarization D_{NN} are given. In agreement with earlier measurements from DISTO. We find a strong contribution of K exchange in the framework of the Laget model. For backward Λs we find a weakening of the depolarization that does not agree with DISTO. Although this effect is expected, more data is desirable to draw a final conclusion on that matter.

We applied a method to extract the $p\Lambda$ effective scattering length from the shape of the final state interaction. The experimental precision of the COSY-TOF detector surpasses the error inherent to the method. To extract the spin triplet scattering length, the K analyzing power was studied. However, the symmetric contribution from S and P wave interference close to threshold was found to be too low to perform the measurement with the available amount of data. A theoretical explanation is pending and would be aided by higher statistical precision of the measurement.

7 Outlook

By the end of this year we will improve the statistics for $p_b = 2.95\,\mathrm{GeV}/c^2$ and will measure at $p_b > 3.15\,\mathrm{GeV}/c^2$. A beam time at $p_b = 2.7\,\mathrm{GeV}/c^2$ already yielded 200,000 $pK\Lambda$ events. The different beam momenta will give important insight into the influence of N^* resonances. A first look into the new data indicates a reduced N^* influence and that the symmetric contribution to the K analyzing power is about 15%. Therefore, it will be possible to measure the spin triplet scattering length. Furthermore, the cusp effect $p_b = 2.7\mathrm{GeV}/c^2$ seems to be strongly reduced so the energy dependence will be an additional aspect in our efforts to to study the coupled channel effects.

References

1. A. Gasparyan, J. Haidenbauer, C. Hanhart and J.M. Speth, Phys.Rev. **C96**, (2004) 034006
2. M. Maggiora, Nucl.Phys. **A691**, (2001) 329-335
3. D. Besset *et al.*, Nucl.Instrum.Meth. **166**, (1979) 515-520
4. J.M. Laget, Phys.Lett. **B259**, (1991) 24-28
5. T.A. Rijken, V.G.J. Stoks and T.Yamamoto, Phys.Rev. **C59**, (1999) 21-40
6. J. Haidenbauer and U.G. Meissner, Phys.Rev. **C72**, (2005) 044005
7. H. Polinder, J. Haidenbauer and U.G. Meissner, Nucl.Phys. **A779**, (2006) 244-266
8. A. Budzanowski *et al.*, Phys.Lett. **B687**, (2010) 31-35
9. A. Gasparyan, J. Haidenbauer, C. Hanhart and J.M. Speth, Phys.Rev. **C72**, (2005) 034006